

Microstructure fabrication and transport through quantum dots

J. N. Randall, M. A. Reed, T. M. Moore, R. J. Matyi, and J. W. Lee^{a)}
Central Research Laboratories, Texas Instruments Incorporated, Dallas, Texas 75265

(Received 27 May 1987; accepted 26 August 1987)

We report the microfabrication techniques used to produce devices which study electronic transport through quantum dots. Molecular-beam epitaxy, electron-beam lithography, and reactive ion etching have been utilized in this effort. The minimum physical lateral size of the dots reported here is $0.1 \times 0.2 \mu\text{m}$. Transport shows some degradation in I - V characteristics with respect to much larger resonant tunneling diodes. Current densities observed suggest the electrical size of diodes is smaller than the physical size. A surface depletion region of 500 \AA may account for this effect. Telegraph noise is observed as a result of single electron trapping in the structure. No clear evidence of lateral quantization has been observed.

I. INTRODUCTION

The progress towards smaller and faster electronics will eventually push devices into regimes where quantum effects will dominate transport.^{1,2} Resonant tunneling diodes have been studied which show strong quantum effects in electronic transport due to electron confinement in one dimension.^{3,4} In this work we demonstrate resonant tunneling diode structures which we use to attempt to study lateral quantization effects. The microfabrication techniques which are used to create quantum dot structures which have direct electrical contact are described. Electronic transport through small arrays and single quantum dots is demonstrated. This type of device should allow the study of several different aspects of electronic transport on the quantum level and will also help understand some of the processing issues involved with producing quantum size effect devices.

II. MICROFABRICATION APPROACH

In order to study electron transport through quantum dots we have adopted a microfabrication approach which is summarized in Fig. 1. After molecular-beam epitaxy (MBE) growth of a resonant tunneling diode structure, an electron-beam (e-beam) lithography step is used to define an ensemble of quantum dots. A liftoff process will leave metal dots that will serve the dual purposes of an etch mask and top-side Ohmic contact. A highly anisotropic reactive ion etching (RIE) process will proceed through the quantum well structure, producing the desired lateral confinement of the GaAs quantum wells. A planarizing layer of dielectric material will be deposited, and then etched back to uncover the top-side dot contacts. Finally, a gold layer will connect the quantum dots with a bond pad. Details of these steps are given in the following sections.

III. MBE GROWTH

The resonant tunneling structure was grown by MBE in a Riber 2300 on a 2-in. n^+ (Si-doped, Sumitomo) GaAs substrate oriented 2° off the $\langle 100 \rangle$. An indium-free, direct radiative substrate heater was used. Following the growth of a $0.5\text{-}\mu\text{m}$ -thick Si-doped ($2 \times 10^{18} \text{ cm}^{-3}$) GaAs buffer layer at 620°C , the doping was graded down to $< 10^{16} \text{ cm}^{-3}$ over a 200 \AA distance. The undoped tunneling structure consisted

of (1) a $50\text{-}\text{\AA}$ -undoped GaAs spacer layer; (2) a $50\text{-}\text{\AA}$ - $\text{Al}_{0.27}\text{Ga}_{0.73}\text{As}$ barrier; and (3) a $50\text{-}\text{\AA}$ -undoped GaAs quantum well. Following the growth of the second $50\text{-}\text{\AA}$ - $\text{Al}_{0.27}\text{Ga}_{0.73}\text{As}$ barrier and spacer layer, the doping was graded back up to $2 \times 10^{18} \text{ cm}^{-3}$ and the top contact ($0.5 \mu\text{m}$) was grown.

IV. E-BEAM LITHOGRAPHY

High-resolution e-beam lithography was accomplished using a standard JEOL JSM-35 scanning electron microscope (SEM) modified for e-beam lithography. The lithography modification consists of a Tracor Northern TN-5500 x-ray analysis system with a digital imaging package, stage automation, and beam blanking.⁵ The patterns are stored as a 256×256 array and written as a 1024×512 array. The dose in each pixel is controlled by varying the duration of

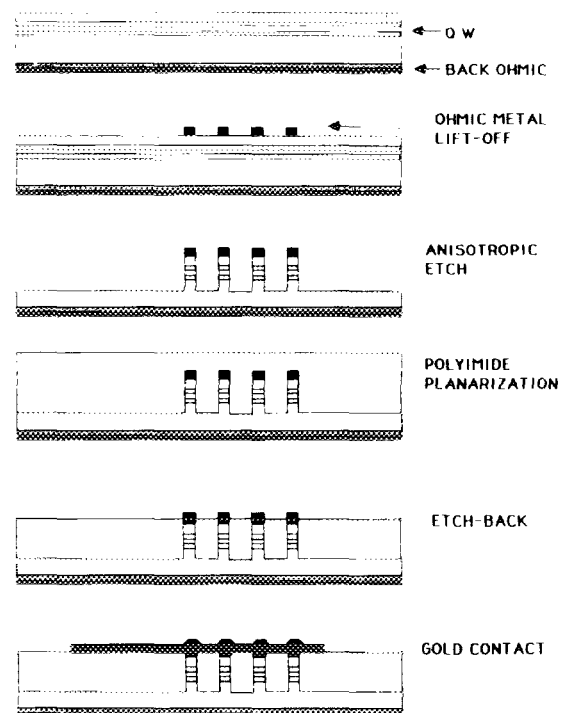


FIG. 1. Schematic of fabrication sequence of quantum dot devices.

exposure. The beam energy was set at 39 keV and the current for these exposures was typically 3 pA.

Using stage automation, several patterns were written at a time, adjacent to a previously defined metal pattern which served as a registration guide and focusing pattern. Three different sized dots were defined which were nominally 0.25, 0.15, and 0.1 μm in diameter. Each of the different sized dots were exposed as single dots as well as arrays of 4, 9, and 16 dots on 1- μm centers. The dose required for exposure of the different sized dots ranged from $\sim 50 \mu\text{C}/\text{cm}^2$ for the 0.25- μm dots to over $200 \mu\text{C}/\text{cm}^2$ for the 0.1- μm dots. This discrepancy is only partially explained by standard proximity effects.⁶

The resist system used was a polymethylmethacrylate (PMMA) bilayer consisting of 1000 \AA of 950 000 molecular weight (MW) material as a top layer and 3000 \AA of 450 000 MW PMMA underneath. This system is designed to give undercut profiles which facilitate liftoff pattern transfer.⁷ The resist was developed in a 60/40 mixture of methylisobutylketone and isopropyl alcohol at room temperature.

The metal layer patterned by the e-beam lithography must serve the dual purpose of RIE etch mask and Ohmic contact. For this purpose we use a three-layer metallization consisting of 500- \AA Au/Ge, 150- \AA Ni, and 600- \AA Au. These layers were evaporated consecutively in the stated order onto the e-beam exposed samples. The liftoff process was completed by soaking the samples in boiling acetone and then applying a vigorous acetone spray.

V. REACTIVE ION ETCHING

The transfer of the metal dot pattern into the semiconducting material which contains the quantum well structure demands both extremely high anisotropy and reasonably low etch rate of the metal mask. The metal dots must not only physically survive the etch process but also must preserve their Ohmic contact characteristics.

The etch process developed used BCl_3 as an etch gas flowing at 30 sccm with a pressure of 30 mTorr. The power delivered by a 13.56-MHz rf generator was $1 \text{ W}/\text{cm}^2$ and the self-bias potential was 300 V. The RIE chamber was custom built at Texas Instruments. A Si wafer was used as the surface of the driven electrode on which the samples were placed. The etch rate of GaAs for these conditions was nominally 350 $\text{\AA}/\text{min}$. The etch rate of Au was $\sim 20 \text{\AA}/\text{min}$. These conditions were selected because they provided excellent anisotropy while maintaining reasonable selectivity. An example of quantum dot structures successfully etched with this technique is seen in Fig. 2.

VI. CONTACT

In order to make contact to the tops of the columns polyimide was spun on the wafer, cured, and then etched back by oxygen RIE until the tops of the columns were exposed. The endpoint to the etching was accomplished by iterative etching and viewing in a SEM. A gold contact layer was lifted off which provided bonding pads for contact to either single dots or arrays of them.

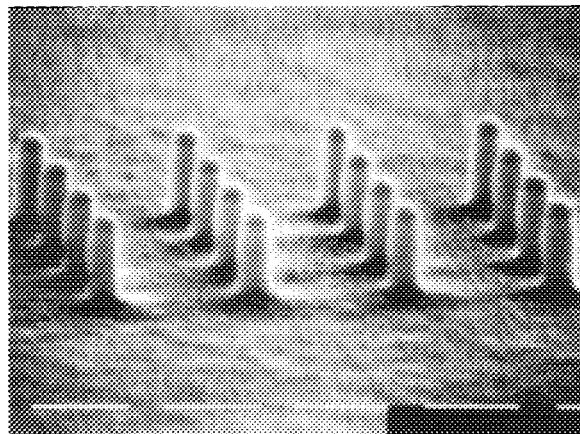


FIG. 2. Scanning electron micrograph of anisotropically etched columns containing quantum dots.

VII. TRANSPORT MEASUREMENTS

Figure 3 shows the I - V characteristic at room temperature of a large area ($2 \times 2 \mu\text{m}$) resonant tunneling diode fabricated by chemical mesa etching from the MBE material discussed above. The structure exhibits a 1.6:1 peak-to-valley tunnel current ratio and a current density at a resonance of $1.6 \times 10^4 \text{ A}/\text{cm}^2$.

Figure 4 shows a similar I - V characteristic of a single quantum dot resonant tunneling structure at 300 K. The lateral dimensions of this single dot structure is $0.15 \times 0.25 \mu\text{m}$. The structure clearly shows negative differential resistance (NDR), though the peak-to-valley is degraded from the large area structure, probably due to process damage. The I - V clearly exhibits a "noise" that is far above the system background noise. The origin of this noise is the so-called "single electron switching" phenomena⁸ that has been observed in narrow Si metal-oxide-semiconductor field-effect transistor wires. Traps in or near the narrow conduction channel and near the Fermi level can emit or capture electrons with a temperature-dependent characteristic time. This can be seen in Fig. 5, where the switching is more well

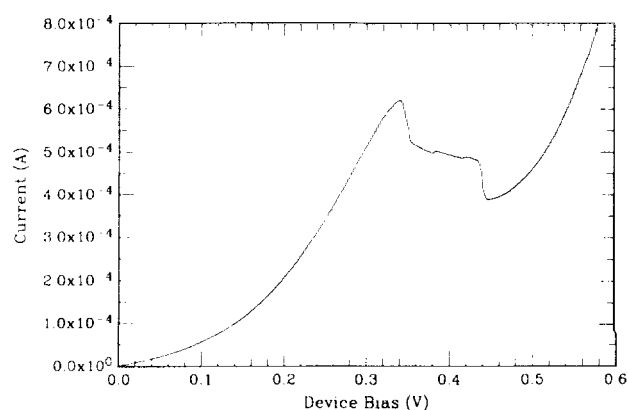


FIG. 3. I - V trace at room temperature of $2 \times 2 \mu\text{m}$ resonant tunneling diode which is fabricated from same vertical epitaxial structure as the quantum dot devices.

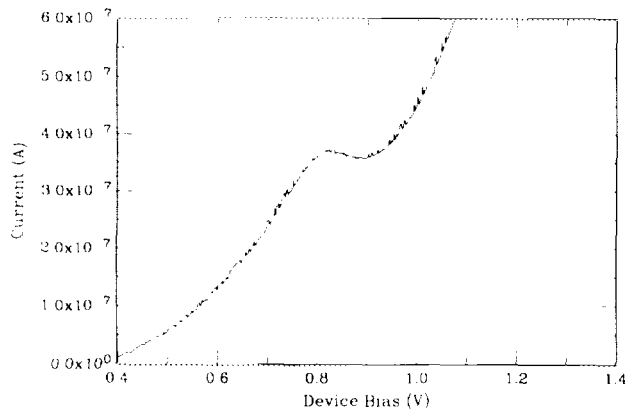


FIG. 4. I - V characteristics at 300 K of a single quantum dot which has lateral dimensions $0.25 \times 0.15 \mu\text{m}$.

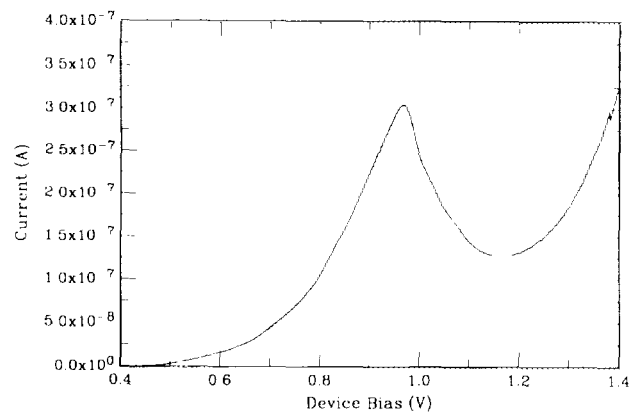


FIG. 6. I - V trace at 4.2 K of a single quantum dot which has lateral dimensions $0.25 \times 0.15 \mu\text{m}$.

defined at 100 K than at 300 K due to the fast thermal activation of the traps at 300 K. The lowering of specific traps through the Fermi level is also clearly evident (at 0.6, 0.8–0.85, 1.0–1.1 V). These traps can be “frozen out,” as we see in Fig. 6 where the temperature has been lowered to 4.2 K.

Figures 7 and 8 show a time-dependent trace of the current through this device at fixed bias voltage (i.e., fixed voltages on Fig. 5) at $T = 84 \text{ K}$. Figure 7 shows the switching between two discrete resistance states at $V = 0.71 \text{ V}$, implying the trapping and detrapping of single electrons onto the same trap. At higher device bias (Fig. 8; 0.875 V), the switching due to a number of traps is evident.

It seems unlikely that such effects can be seen for the physical dimensions ($0.15 \times 0.25 \mu\text{m}$) of the structure. However, the effects of depletion at the etched mesa surfaces has not been taken into account. Taking the observed current at resonance and assuming that the current density must be the same as in the large area device (assuming that the switching is a perturbation), we calculate that the effective (circular) conduction path diameter is $\sim 500 \text{ \AA}$, consistent with the observation of the switching phenomena. This implies a depletion layer of $\sim 500 \text{ \AA}$. However, transport was also seen in an array of dots 2000 by 1000 \AA , suggesting a depletion layer smaller than 500 \AA .

At these lateral dimensions, splitting of the quantum well

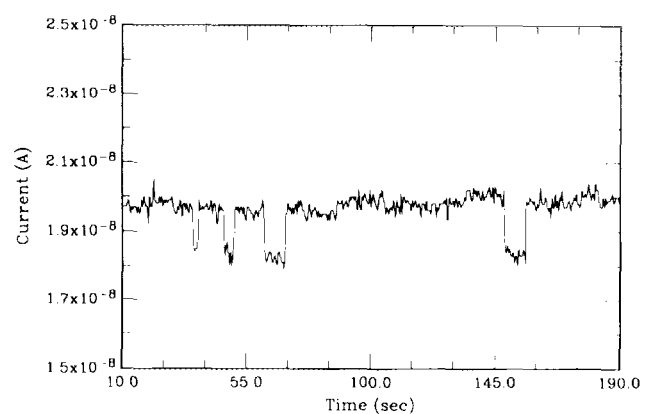


FIG. 7. Time dependent current fluctuations at a fixed bias of 0.71 V of a single quantum dot which has lateral dimensions $0.25 \times 0.15 \mu\text{m}$. $T = 84 \text{ K}$.

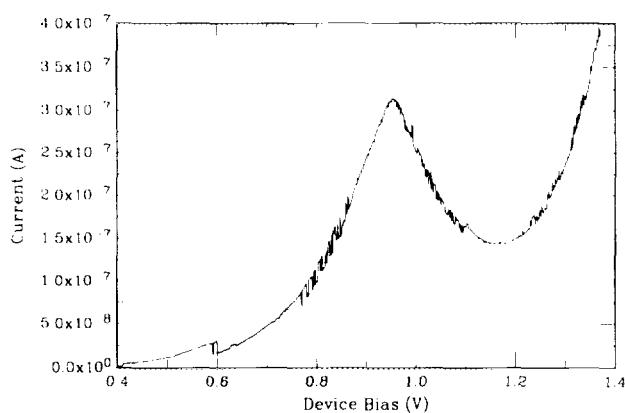


FIG. 5. I - V trace at 100 K of a single quantum dot which has lateral dimensions $0.25 \times 0.15 \mu\text{m}$.

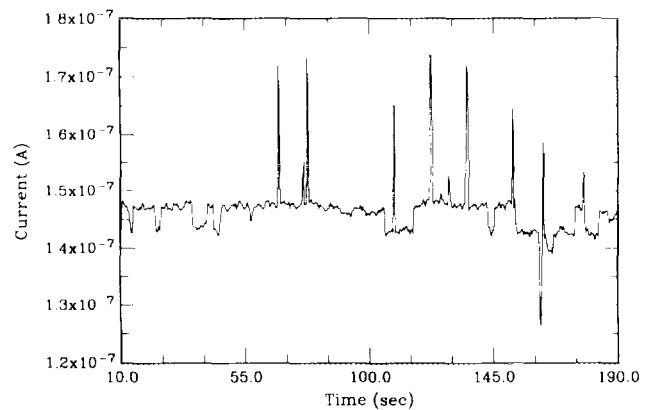


FIG. 8. Time-dependent current fluctuations at a fixed bias of 0.875 V of a single quantum dot which has lateral dimensions $0.25 \times 0.15 \mu\text{m}$. $T = 84 \text{ K}$.

resonance due to lateral size quantization should be observable. High-resolution scans similar to Fig. 6 have been performed, but no definite indications of lateral quantization have yet been observed.

VIII. CONCLUSIONS

We have demonstrated a successful microfabrication technique for studying electronic transport in quantum dots. Transport through the quantum dots shows single electron trapping events. While no clear evidence of lateral quantization has been observed, we believe that these microfabrication techniques should be able to yield dots sufficiently small to produce this effect.

ACKNOWLEDGMENTS

The authors wish to thank Randy Thomason, Doug Schultz, Pam Stickney, and Robert Aldert for technical assistance. We also are indebted to Bob Bate and Bill Frensley

for valuable advice and discussions. This work was sponsored by the Army Research Office.

^{a1} Present address: Kopin Corp., 695 Myles Standish Blvd., Taunton, MA 02780.

¹R. T. Bate, *Superlattices Microstructures* **2**, 9 (1986).

²Artificially Structured Materials, report of a panel of the Solid State Sciences Committee, National Research Council (National Academy, Washington, D.C. 1985).

³L. L. Chang, L. Esaki, and R. Tsu, *Appl. Phys. Lett.* **24**, 593 (1974).

⁴T. C. L. G. Sollner, W. D. Goodhue, P. E. Tannenwald, C. D. Parker, and D. D. Peck, *Appl. Phys. Lett.* **43**, 588 (1983).

⁵P. E. Russel, T. North, and T. M. Moore, in *Microbeam Analysis—1986*, edited by A. D. Romig and W. F. Chambers (San Francisco, San Francisco, 1986), pp. 663–666.

⁶J. A. Oro, Ph.D. thesis, Electrical Engineering Department, University of Houston, 1987.

⁷M. J. Rooks, P. McEuen, S. Wind, and D. E. Prober, *Mater. Res. Soc. Symp. Proc.* **76**, 55 (1987).

⁸K. S. Ralls, W. J. Skocpol, L. D. Jackel, R. E. Howard, L. A. Fetter, R. W. Epworth, and D. M. Tennant, *Phys. Rev. Lett.* **52**, 228 (1984).